ACS OMEGA

http://pubs.acs.org/journal/acsodf

Article

Experimental Measurement and Thermodynamic Modeling of the Wax Disappearance Temperature (WDT) for a Quaternary System of Normal Paraffins

Fatemeh Shariatrad, Jafar Javanmardi,* Ali Rasoolzadeh, and Amir H. Mohammadi*

Cite This: *ACS Omega* 2022, 7, 16928−16938

Read Online

ACCESS | Metrics & More | Article Recommendations

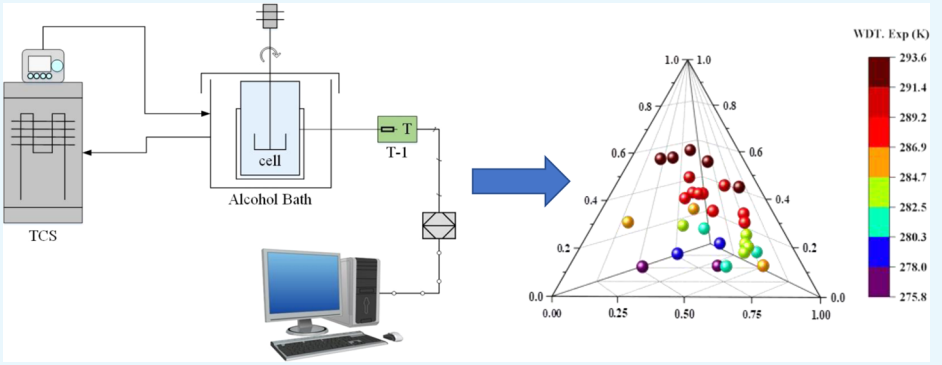

ABSTRACT: Normal paraffin (*N*-alkane)-based wax is well known as a severe problem in petroleum production, transportation, and processing. Implementing suitable solutions for wax-related problems requires vast technical knowledge and investigation of the wax disappearance temperature (WDT) of multicomponent systems in petroleum-dominated systems. In this study, the WDTs of a quaternary system comprising different mixtures of *n*-undecane + *n*-tetradecane + *n*-hexadecane + *n*-octadecane were measured using a visual-based diagnosis apparatus under atmospheric pressure. On the other hand, the WDTs of the studied systems are predicted by applying a solid solution model without any adjustable parameter. Two approaches namely $\gamma-\varphi$ and $\gamma-\gamma$ are assessed. In the $(\gamma-\varphi)$ approach, perturbed-chain statistical associating fluid theory (PC-SAFT) is applied for liquid phase modeling, while the solid phase is described using different activity coefficient models. In the $(\gamma-\gamma)$ approach, nonidealities of both the liquid and solid phases are investigated using different combinations of activity coefficient models such as ideal solution, regular solution theory, predictive Wilson, predictive UNIQUAC, and UNIFAC. Comparison of experimental data and thermodynamic modeling results indicates that applying the predictive UNIQUAC model for describing the nonideality of the solid phase and the regular solution model for the liquid phase is the best combination for the aforementioned system with the average absolute deviation (AAD) of 0.8 K.

1. INTRODUCTION

It is estimated that oil extraction growth will be continued until 2040.[1] For enhancing oil production over a short period of time, there should be a significant improvement in areas related to extraction/production science and technology. It should be particularly mentioned that there are a significant number of oil fields that contain waxy compounds with high molecular weights. Under certain thermodynamic circumstances, *n*-alkanes deposition can decrease oil production efficiency by crystallizing on equipment.[2−4] To vanquish the serious adversities in the way of oil production and processing and predominantly its transportation, detailed comprehension of the solid−liquid equilibria of waxy oils is required. Hereupon, studying the behaviors of *n*-alkanes with the measurement and prediction of the wax appearance temperature (WAT) is of interest. WAT describes a temperature at which the initial crystal of wax starts to precipitate when cooling a liquid mixture.[5] Based on previous research studies,[6−8] WAT is not a reliable parameter because of weak reproducibility, repeatability, and its dependency on measurement conditions. Moreover, WAT is more dependent on the kinetics of crystal formation like cooling rates or experimental measurement techniques, so the experimental conditions and the measurement techniques have great impacts on it; in other words, it is a path function property. On the other hand, wax

Received: December 15, 2021
Accepted: March 16, 2022
Published: May 13, 2022

https://doi.org/10.1021/acsomega.1c07072
ACS Omega 2022, 7, 16928−16938

disappearance temperature (WDT) is a temperature wherein the last tiny particles of wax crystals break down in the liquid phase on heating and represents an actual equilibrium state, a point function property.[6,9−11] Several studies indicate that the difference between the measured WAT and WDT by one method can be considerable.[12,13]

Researchers have conducted different experimental studies on WATs and WDTs of mixtures of alkanes and waxy crude oils using different methods such as light transmittance,[12] cross-polar microscopy (CPM),[8] differential scanning calorimetry (DSC),[14] and viscometry.[15] For example, Daridon et al.[16] utilized a high-pressure cell mounted on a polarizing microscope to measure WDT for several *n*-alkane mixtures from *n*-C_{13} to *n*-C_{24} under pressures up to 100 MPa. Due to the limitations of conventional laboratories, although this apparatus is highly accurate, it is expensive and difficult to access. Pauly et al.[17] investigated the quantity and composition of the precipitated wax in five mixtures of an *n*-C_{10} + (*n*-C_{24} + *n*-C_{25} + *n*-C_{26}) quaternary system at different temperatures under a WAT applying chromatographic technique and filtration. They also measured the WAT of each mixture at atmospheric pressure. It is evident that due to the quaternary system's complexity, WAT measuring for only five different mixtures of a quaternary system is not sufficient to estimate system behavior. Mansourpoor et al.[18] experimentally measured the WATs of 12 samples of Iranian crude oils and condensates using DSC and viscometry methods. They used an artificial neural network (ANN) model to estimate the WDTs of crude oils. They also introduced a precise correlation that determines the WDT with good agreement with laboratory data. Due to the expensiveness, time consumption, and difficulty of the experimental approaches, the development of thermodynamic models can help operating engineers predict wax deposition conditions in production facilities, oil transportation pipelines, or process equipment. Currently, there are two viewpoints for thermodynamic modeling of wax deposition. First, the solid solution (SS) approach states that only one solid phase of wax containing miscellaneous hydrocarbon components can exist.[19,20] Second, the multi solid (MS) approach states that the wax phase is composed of several pure solid phases.[21] Won[19] developed one of the initial SS models for wax deposition. In this model, for the description of the solid phase, a modified regular solution theory is employed, and the Soave−Redlich−Kwong (SRK) equation of state (EoS)[22] is applied for vapor−liquid equilibria calculations. Also, Won corrected fusion temperatures and fusion enthalpies of pure *n*-alkanes as a function of molecular weights. Pedersen et al.[23] developed Won's model and, for WAT prediction, calculated the activity coefficients of both solid and liquid phases from the modified regular solution theory. Coutinho and Stenby[20] surveyed the orthorhombic solid phase by Wilson's model. Afterward, Coutinho et al.[24] presented a modified UNIQUAC model[24] to describe the orthorhombic solid-phase in solid−liquid equilibria of hydrocarbon mixtures. In comparison with Wilson's model,[25] the UNIQUAC model[25] was more practical. They tested a combination of UNIFAC and Flory free-volume approaches[25] to describe the nonideality behavior of the liquid phase, but the results are not satisfying enough. Ji et al.[6] presented a thermodynamic model according to the SS theory,[19] which calculates the WDT and determines the quantity and composition of precipitated wax. According to their model, the UNIQUAC excess Gibbs energy model[25] is used for solid fugacity calculation in the solid−liquid equilibrium. Also, to obtain fugacity in the vapor−liquid equilibrium, the SRK and Peng-Robinson (PR) EoSs[22,26] are employed. New correlations are provided for heat capacity and fusion properties, which consider the impact of even or odd *n*-paraffin carbon numbers to achieve more accurate results. They also measured the WDTs of some binary systems to validate their proposed correlations. Esmaeilzadeh et al.[27] used combinations of different activity coefficient models to predict the WATs of some binary, ternary, quaternary, and multicomponent systems. They realized that when the carbon numbers of system components are consecutive, the SS model[19] is more accurate, and the MS model[21] predicts WAT lower than the actual value in general. Aftab et al.[11] conducted some experiments to measure the WDTs of two different ternary systems containing *n*-C_{11} + *n*-C_{16} + *n*-C_{18} and *n*-C_{14} + *n*-C_{16} + *n*-C_{18} by a visual method. They also used two different SS models for thermodynamic modeling. In the first method, PC-SAFT EoS[28] and the predictive version of the UNIQUAC (p.UNIQUAC) activity coefficient model[24] are used to estimate the nonideality of the liquid and solid phases, respectively. In the second method, they assumed that both phases could be described incorporating different activity coefficient models. The results indicate that the combination of regular solution theory[19] for the liquid phase with the predictive version of the Wilson (p.Wilson)[20] for the solid phase leads to the best precision relative to other activity coefficient models (AADs of 0.48 and 0.76 K for *n*-C_{11} + *n*-C_{16} + *n*-C_{18} and *n*-C_{14} + *n*-C_{16} + *n*-C_{18} systems, respectively). Parsa et al.[29] measured the WDTs of three different binary systems (*n*-C_{11} + *n*-C_{18}, *n*-C_{16} + *n*-C_{18}, *n*-C_{14} + *n*-C_{16}) and compared experimental WDTs with the results of thermodynamic models based on SS.[19] The best combination of the activity coefficient models for the (*n*-C_{11} + *n*-C_{18}) and (*n*-C_{16} + *n*-C_{18}) systems was obtained by the ideal solution theory[25] for the liquid phase and p.UNIQUAC model[24] for the solid phase (AADs of 0.22 and 0.32 K, respectively). The *n*-C_{14} + *n*-C_{16} system had the lowest AAD value of 0.43 K with the ideal solution[25] + p.Wilson package.[20]

There are a few experimental studies on WATs and WDTs of *n*-alkanes in quaternary systems.[16,17] However, no extensive and methodical studies have yet been performed on quaternary systems. This work aims to investigate a quaternary system in various compositions accurately and validate different thermodynamic models to predict the WDT. In this study, WDTs of a quaternary system containing *n*-C_{11} + *n*-C_{14} + *n*-C_{16} + *n*-C_{18} were experimentally measured using a visual-based diagnosis apparatus under the atmospheric pressure (about 0.9 bar). Then, a thermodynamic model based on the SS model[19] is proposed to determine the WDT of the studied quaternary system. For describing the liquid phase, PC-SAFT EoS[28] and different activity coefficient models such as ideal behavior,[25] regular solution theory,[19] and UNIFAC[25] are applied. The solid phase degree of nonideality behavior is characterized by ideal behavior,[25] regular solution theory,[19] p.Wilson,[20] p.UNIQUAC,[24] and UNIFAC[25] activity coefficient models. Eventually, the modeling results are compared with the experimental data, and then the best combination of thermodynamic sets for the liquid and solid phases, which can precisely determine the experimental results, are introduced.

https://doi.org/10.1021/acsomega.1c07072
ACS Omega 2022, 7, 16928−16938

2. RESULTS AND DISCUSSION

The reliability of the WDT measurement technique used in this study was confirmed previously.[29] WDTs of 30 mixtures of the n-C_{11} + n-C_{14} + n-C_{16} + n-C_{18} quaternary system were experimentally measured. The composition of these mixtures is reported in Table 1.

Table 1. Experimental Data of WDTs at Atmospheric Pressure (about 0.9 bar) for the n-C_{11} + n-C_{14} +n-C_{16} + n-C_{18} Quaternary System Depending on Weight Fractions[a]

	weight fraction				
mixture number	n-$C_{11}H_{24}$	n-$C_{14}H_{30}$	n-$C_{16}H_{34}$	n-$C_{18}H_{38}$	Exp. WDT (K)
1	0.3114	0.2224	0.4124	0.0538	275.8
2	0.0752	0.5791	0.2404	0.1052	276.8
3	0.1347	0.4032	0.3161	0.1460	278.9
4	0.2477	0.1851	0.4023	0.1649	280.0
5	0.2857	0.0476	0.5476	0.1191	281.8
6	0.1036	0.2518	0.5443	0.1003	282.4
7	0.1830	0.2340	0.3401	0.2429	282.4
8	0.2556	0.0612	0.4833	0.1999	282.9
9	0.1925	0.1048	0.5270	0.1757	283.0
10	0.2439	0.2927	0.2195	0.2439	283.1
11	0.1170	0.1504	0.5773	0.1553	284.4
12	0.1291	0.1211	0.5748	0.1750	284.5
13	0.1025	0.1115	0.6826	0.1034	285.1
14	0.1029	0.5379	0.0718	0.2874	286.0
15	0.3075	0.1963	0.1925	0.3037	286.2
16	0.4413	0.1019	0.1103	0.3465	286.3
17	0.1470	0.0625	0.4778	0.3127	287.0
18	0.0747	0.1969	0.3895	0.3389	287.2
19	0.1250	0.2001	0.2714	0.4035	287.3
20	0.3354	0.1573	0.1360	0.3713	287.5
21	0.0910	0.0957	0.5266	0.2866	287.6
22	0.1404	0.1788	0.2798	0.4010	287.6
23	0.2374	0.2290	0.1695	0.3641	288.4
24	0.1197	0.0852	0.3563	0.4388	289.6
25	0.2102	0.1748	0.1542	0.4608	291.1
26	0.0732	0.0488	0.4390	0.4390	291.5
27	0.0765	0.1133	0.2616	0.5486	292.1
28	0.2406	0.1036	0.0799	0.5760	293.3
29	0.0636	0.2920	0.0796	0.5648	293.5
30	0.1505	0.2159	0.0768	0.5568	293.6

[a]Expanded uncertainty U_c is U_c (T) = 0.1 K, U_c (w) = 0.0001, and U_c (P) = 0.1 bar (0.95 level of confidence).

Light n-alkanes play an important role in the oil industry. For example, they are used as the feed of the isomerization process. C_4−C_7 and C_7−C_{15} n-alkanes are used to produce high octane gasoline and diesel fuel, respectively. C_{15+} n-alkanes make up greater than 80 wt % wax and commonly, distillate cuts have large amounts of these components, which their probable presence in the feed of isomerization causes the freezing point of products to be higher than the standard level. According to the 8th and 17th mixtures or the 9th and 21st mixtures in Table 1, it can be seen that when the weight fractions of n-C_{14} and n-C_{16} are approximately fixed and the weight fraction of n-C_{18} is increased, the WDTs in mixture numbers 17 and 21 are increased. This observation reflects the fact that increasing the weight fractions of the heavier components will cause an increase in the WDT.[11] This has been mentioned in Section 4.3.

Fifteen different sets of activity coefficient models and five various sets of the PC-SAFT EoS[28] + activity coefficient models were applied to calculate WDTs without any adjustable parameters. The results of using various activity coefficient models including ideal behavior,[25] regular solution theory,[19] UNIFAC,[25] and PC-SAFT EoS[28] for the liquid phase and combining them with the ideal behavior,[25] regular solution theory,[19] p.Wilson,[20] p.UNIQUAC,[24] and UNIFAC[25] models for the solid phase were investigated by calculating the average absolute deviation (AAD) with and without considering the solid−solid phase transition. The calculated AADs (K) have been classified from low to high values in Table 2.

Table 2. Average Absolute Deviations (AADs) for WDT Prediction by 20 Various Combinations of Models for Investigated Quaternary Mixtures[a]

			AAD[a] (K)	
no	liquid phase	solid phase	with solid−solid transition	without solid−solid transition
1	regular solution[19]	p.UNIQUAC[24]	0.8	0.8
2	ideal solution[25]	p.UNIQUAC[24]	0.9	0.8
3	UNIFAC[25]	p.UNIQUAC[24]	0.9	0.9
4	PC-SAFT[28]	p.UNIQUAC[24]	0.9	0.8
5	regular solution[19]	p.Wilson[20]	1.0	1.0
6	ideal solution[25]	p.Wilson[20]	1.0	1.1
7	UNIFAC[25]	p.Wilson[20]	1.0	1.0
8	PC-SAFT[28]	p.Wilson[20]	1.2	1.2
9	UNIFAC[25]	regular solution[19]	2.8	2.8
10	ideal solution[25]	regular solution[19]	2.9	2.9
11	PC-SAFT[28]	regular solution[19]	2.9	2.9
12	regular solution[19]	regular solution[19]	2.9	3.0
13	UNIFAC[25]	ideal solution[25]	4.0	4.3
14	UNIFAC[25]	UNIFAC[25]	4.1	4.4
15	PC-SAFT[28]	UNIFAC[25]	4.2	4.5
16	ideal solution[25]	ideal solution[25]	4.2	4.5
17	ideal solution[25]	UNIFAC[25]	4.2	4.5
18	PC-SAFT[28]	ideal solution[25]	4.2	4.5
19	regular solution[19]	ideal solution[25]	4.2	4.5
20	regular solution[19]	UNIFAC[25]	4.3	4.6

[a]$\mathrm{AAD}(K) = \frac{1}{n}\sum_{i=1}^{n} |\mathrm{WDT}_i^{\mathrm{Cal}} - \mathrm{WDT}_i^{\mathrm{Exp}}|$.

Comparing rows 1−4 of Table 2 illustrates that the liquid-phase behavior is close to the ideal solution because by changing the activity coefficient models or using PC-SAFT EoS[28] for describing the liquid phase while the p.UNIQUAC model[24] is applied to characterize the solid-phase behavior, outputs are not varied significantly. This result is in line with the formerly published literature.[11,29] According to Table 2, it can be observed that the most suitable sets of activity coefficient models that lead to the lowest deviation are the regular solution theory[19] and p.UNIQUAC model[24] for the liquid and solid phases, respectively. The reason is that the

https://doi.org/10.1021/acsomega.1c07072
ACS Omega 2022, 7, 16928−16938

p.UNIQUAC model[24] is a modified version of the UNIQUAC[25] to calculate solid−liquid equilibria of alkanes and can accurately describe the nonidealities of the paraffinic solid solutions and can predict the phase behavior of complex hydrocarbon mixtures at low and high pressures. The high accuracy of the p.UNIQUAC model[24] is due to several reasons: (1) this model takes into account the size, shape, and structure of the molecules to compute the entropic term. Therefore, this model is suitable for systems containing light to heavy hydrocarbons. (2) It considers the impact of temperature on the molecular interactions in the enthalpic term. (3) It can also determine the phase split, and (4) by assuming the pair interaction energies as a function of the heat of sublimation, it becomes a fully predictive model. Moreover, it can be interpreted from Table 2 that PC-SAFT EoS[28] with no binary interaction parameter can successfully calculate the nonidealities of the liquid phase. The advantage of PC-SAFT EoS[28] is its accuracy in computing the fugacities of the heavy components in the fluid phases.[11,28,30,31] Experimental and predicted (regular solution[19] + p.UNIQUAC[24]) WDTs are depicted in Figure 1.

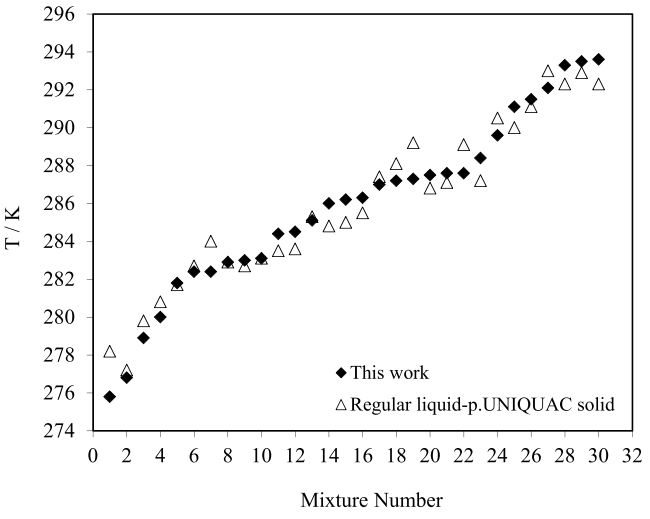

Figure 1. Comparison of experimental and predicted WDTs by regular solution theory[19] for the liquid phase and p.UNIQUAC[24] for the solid phase for different mixtures of the n-C_{11} + n-C_{14} + n-C_{16} + n-C_{18} quaternary system considering the solid−solid phase transition.

Figure 1 shows that the set of the regular solution model[19] for the liquid phase and the p.UNIQUAC model[24] for the solid phase can accurately predict the WDT of the quaternary system studied in this work at a variety of paraffin concentrations. The reason is the superiority of the p.UNIQUAC model[24] in calculating the nonidealities of the solid phase. It can be realized in Figure 2 that using some activity coefficient models such as ideal solution,[25] regular solution theory,[19] and UNIFAC[25] for the solid phase leads to the WDT overestimation.

Furthermore, it is concluded that an accurate calculation of the nonideality of the solid phase is a key parameter for the system studied in this work. It is also seen in Figures 1 and 2 that the p.UNIQUAC[24] and p.Wilson[20] models are suitable for the representation of the solid-phase nonideality, while applying the UNIFAC model[25] for the solid phase has the least precision in predicting the WDT. One of the reasons for the low accuracy of the UNIFAC model[25] is that this model

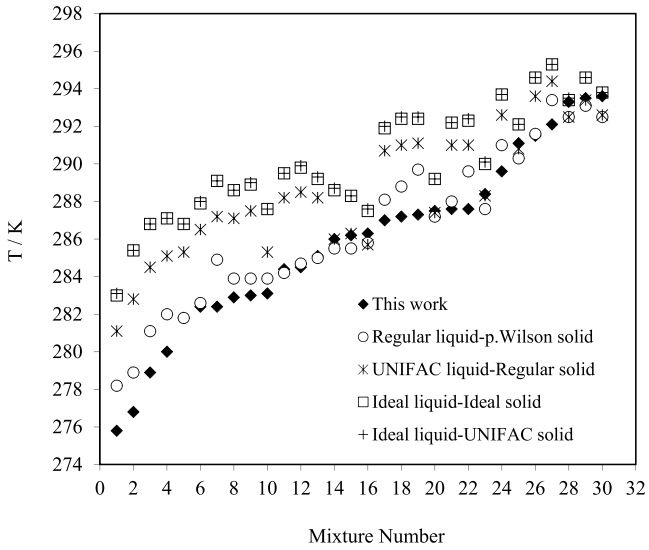

Figure 2. Comparison of experimental and predicted WDTs by different sets of activity coefficient models vs mixture number for the n-C_{11} + n-C_{14} + n-C_{16} + n-C_{18} quaternary system considering the solid−solid phase transition.

was used in its original format and no modification was applied to it. Figure 3 gives a comparison between the experimental

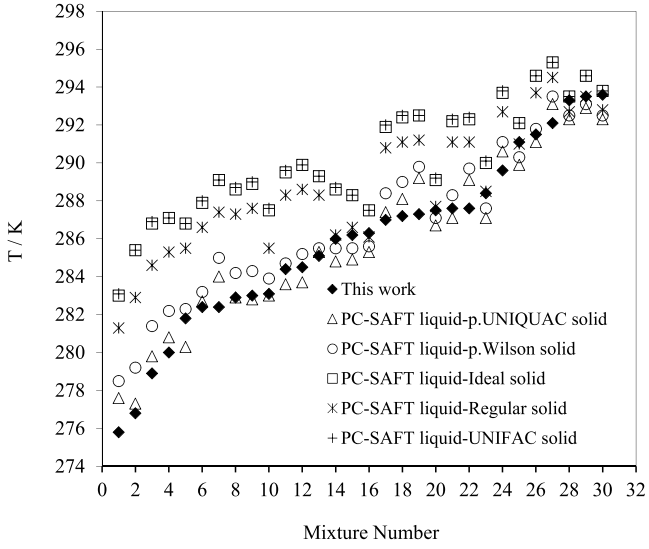

Figure 3. Comparison of experimental and predicted WDTs by PC-SAFT EoS[28] for the liquid phase and different activity coefficient models for the solid phase considering the solid−solid phase transition.

data of the WDT measured in this work and various models that employ PC-SAFT EoS[28] for the liquid phase and different activity models for the solid phase.

Figure 3 depicts that the combination of PC-SAFT EoS[28] and the p.UNIQUAC[24] activity coefficient models gives the best results. The results of the PC-SAFT[28] + p.Wilson[20] package are satisfactory, while using the ideal solution,[25] regular solution,[19] and the UNIFAC[25] models for the solid phase leads to poor results. Figure 4 compares the fractional deviation of WDTs for multiple thermodynamic packages employed in this work.

https://doi.org/10.1021/acsomega.1c07072
ACS Omega 2022, 7, 16928−16938

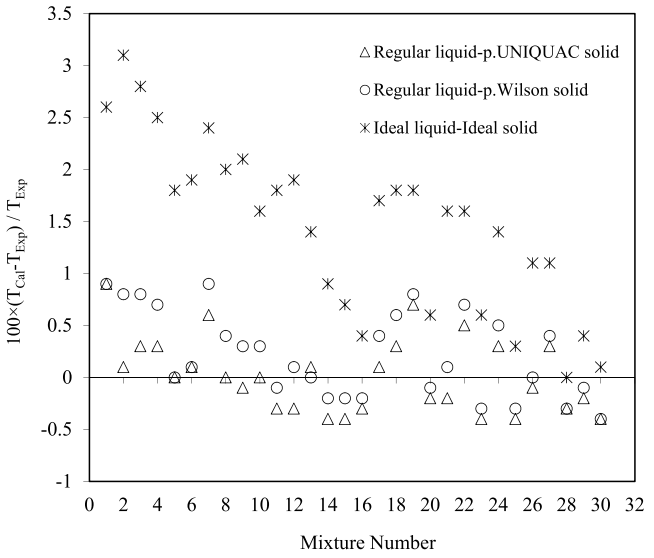

Figure 4. Comparison between fractional deviations of three sets of activity coefficient models in prediction of WDTs.

Figure 4 shows that applying the ideal liquid−ideal solid approach leads to the overestimation of WDTs for all of the mixtures. This is consistent with the results obtained by Ji et al.[6] Both regular solution-p.UNIQUAC[24] and regular solution[19] -p.Wilson[20] combinations result in fractional deviations lower than 1% for all of the mixtures, which indicates the high accuracy of these two models.

By evaluating a variety of activity coefficient models and PC-SAFT EoS,[28] it is concluded that the solid-phase nonideality is a key parameter in the accuracy of a thermodynamic model. Therefore, applying the p.UNIQUAC[24] and p.Wilson[20] activity coefficient models is recommended for the solid phase. Employing various models for the liquid phase leads to approximately the same results. The regular solution[19] + p.UNIQUAC model[24] is the best combination for calculating the WDTs studied in this work. The input parameters of this model are the physical properties, the pressure, and the compositions of the *n*-alkanes in the mixtures. By changing the pressure and composition of *n*-alkanes in the model, it is concluded that the pressure has a negligible impact on WDT, while the compositions of *n*-alkanes have a significant effect on it.

3. CONCLUSIONS

In this study, WDTs of the *n*-undecane + *n*-tetradecane + *n*-hexadecane + *n*-octadecane quaternary system were measured using a visual-based diagnosis apparatus at atmospheric pressure of about 0.9 bar. The WDTs were predicted by combining the different activity coefficient models together and with PC-SAFT EoS[28] for both solid and liquid phases without any adjustable parameter. The investigations indicate that using the different activity coefficient models or PC-SAFT EoS[28] for the liquid phase approximately gives the same results. The UNIFAC model[25] is not appropriate for the explanation of the nonideality of the solid phase, while the p.UNIQUAC[24] and the p.Wilson[20] models show the best performances for the solid phase description in turn. The results indicate that among the investigated activity coefficient models, the use of the p.UNIQUAC model[24] for the solid phase and its combination with the regular solution model[19] for the liquid phase is the most precise one and leads to the best agreement with the experimental data with the AAD of 0.8 K.

4. EXPERIMENTAL SECTION

4.1. Materials. The information and purities of materials used in the experiments are reported in Table 3.

Table 3. Materials Used in This Work

symbol	chemical name	CAS. reg. no.	source	purity (mole fraction)	purification method
n-$C_{11}H_{24}$	*n*-undecane	1120-21-4	Merck	0.99	none
n-$C_{14}H_{30}$	*n*-tetradecane	629-59-4	Merck	0.99	none
n-$C_{16}H_{34}$	*n*-hexadecane	544-76-3	Merck	0.99	none
n-$C_{18}H_{38}$	*n*-octadecane	593-45-3	Merck	0.99	none

4.2. Apparatus. In the current work, the key part of the experimental setup is an equilibrium cell (SS-316) of stainless steel with a 75 cm^3 internal volume that has a window for sample observation. Inside the equilibrium cell, there is a stirrer that makes adequate turbulence for reaching equilibrium. The cell is placed in an ethanol bath with a cooling/heating capability. The regulation of the ethanol bath temperature is accomplished using a manageable circulator (TCS) with scheduling capability (Julabo FP-50). To measure the temperature accurately, a Pt-100 thermometer with an uncertainty of less than 0.1 K is used. An overview of the experimental setup is illustrated in Figure 5.

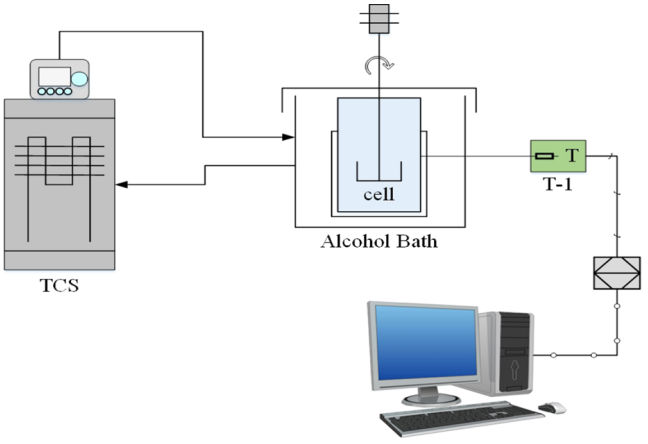

Figure 5. Schematic plan of the experimental setup; T, thermometer and TCS, temperature controller system.

4.3. Experimental Procedure. It has been indicated that using the equilibrium step heating method, the measured WDT can be reliable and reproducible.[6] The visual method has long been used as a technique by researchers.[9,11,29] Some researchers have previously carried out studies on the precision and validity of this method. For example, Parsa et al.[29] showed that there is good agreement between the measured WDTs based on this method and others. They reported that the difference between the measured WDTs of the *n*-C_{14} + *n*-C_{16} binary system by CPM and visual methods would be just up to 0.2 K. Also, their results for experimental melting point

https://doi.org/10.1021/acsomega.1c07072
ACS Omega 2022, 7, 16928−16938

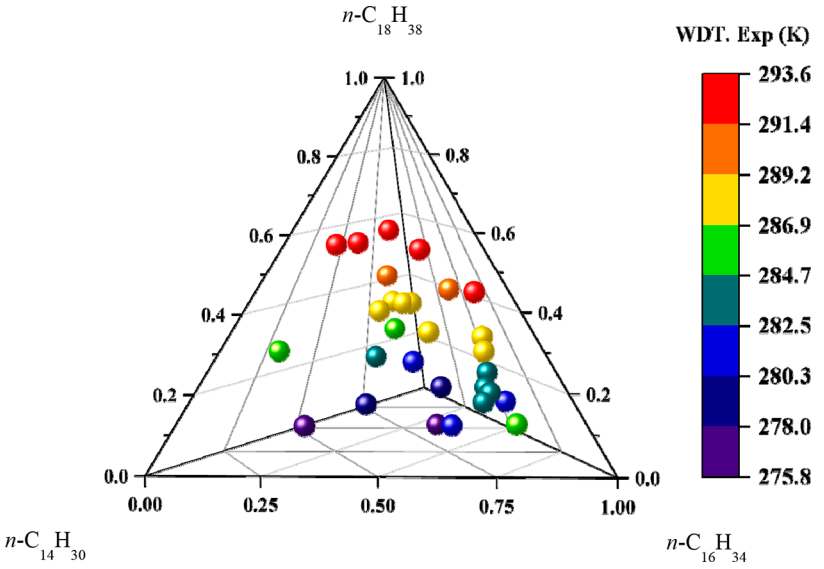

Figure 6. Distribution of experimental data in a tetrahedral plot diagram for the quaternary system.

measurements of pure n-C_{14}, n-C_{16}, and n-C_{18} are in agreement with the NIST Data Bank. Therefore, it has been concluded that the visual method can be a valid technique for measuring the WDTs of multicomponent systems. Hence, in this study, a visual method was used to measure the WDTs of the quaternary system. For each experiment, the quaternary mixture was prepared by a gravimetric method using a digital A&D balance (HR-200) with an accuracy of 0.0001 gr. First, the well-mixed mixture was inserted into the equilibrium cell. After that, the mixture temperature was decreased by approximately 10 °C lower than the predictable WAT. Then, the system temperature was kept constant for an hour using a controllable circulator to achieve a thermodynamically stable state. When wax crystals were formed completely, the heating process was started by raising the temperature of the ethanol bath. A very low heating rate (0.1 K h^{-1}) was applied to make sure that the equilibrium was reached at each step. As the temperature increased, the wax crystals were melted very slowly. This process was carefully observed until the last crystal was redissolved in the mixture, and this exact temperature was determined as the WDT of the mixture. The procedure was repeated twice for each mixture.

Using this method, 30 experimental data were obtained over a wide range of compositions of studied compounds. Weight fractions of all components were changed in the range between 0.04 and 0.70. To enhance the understanding of the distribution of quaternary system compositions, a well-known three-dimensional (3D)-tetrahedral plot was applied, which is a suitable visualization method for quaternary systems in petroleum and mineral sciences.[32] Figure 6 presents this plot for compounds used in this study. According to this figure, the proper distribution of compositions in the studied space is visible. In addition, there is a color scale that indicates the experimental WDTs related to each composition. Based on Figure 6, it is evident that the presence of a higher amount of the n-C_{18} compound, as the heaviest component of the mixtures, causes an increase in the value of the respective WDTs.

4.3.1. Thermodynamic Modeling: γ−γ Approach. In this work, the solid solution model[19] was used because based on studies on the crystal structure, the multisolid approach[21] with the actual behavior of the wax crystal is not consistent.[6] The accuracy of the solid solution model[19] for describing the liquid−solid equilibrium significantly depends on the selection of the appropriate activity coefficient model.[27] The solid−liquid equilibrium of waxy systems can be defined by[11,29]

$$f_i^{l}(T, P, x_i^{l}) = f_i^{s}(T, P, x_i^{s}) \quad i = 1, 2, \ldots N \tag{1}$$

where f_i stands for the fugacity of component "i" in which the superscripts l and s indicate the liquid and solid phases, respectively. f_i is a function of the temperature (T), pressure (P), and mole fraction (x_i). The fugacities of the liquid and solid phases in an n-alkane mixture can be obtained by the $\gamma-\gamma$ approach[11,29]

$$f_i^{l} = x_i^{l}\gamma_i^{l}f_{\text{pure},i}^{l}\exp\left(\int_0^P \frac{v_i^{l}}{RT}\mathrm{d}P\right) \tag{2}$$

$$f_i^{s} = x_i^{s}\gamma_i^{s}f_{\text{pure},i}^{s}\exp\left(\int_0^P \frac{v_i^{s}}{RT}\mathrm{d}P\right) \tag{3}$$

where γ_i and $f_{\text{pure},i}$ are the activity coefficient and fugacity of the pure component "i", respectively. x_i stands for the mole fraction, as mentioned earlier, v_i stands for the molar volume of component "i", T indicates the temperature, as mentioned earlier, and R is the universal gas constant. Prausnitz et al.[25] presented a relationship for the fugacity ratio of the pure liquid and solid states, but due to the effects of the solid phase transition at high temperatures and before fusion, this relationship requires to be slightly changed.[6,10,33] The fugacity ratio of the pure liquid and solid states can be expressed as follows[11,29]

$$\ln\frac{f_{\text{pure},i}^{l}}{f_{\text{pure},i}^{s}} = \frac{\Delta H_i^{\text{tr}}}{RT}\left(1-\frac{T}{T_i^{\text{tr}}}\right) + \frac{\Delta H_i^{\text{f}}}{RT}\left(1-\frac{T}{T_i^{\text{f}}}\right) + \frac{1}{RT}\int_{T_i^{\text{f}}}^{T}\Delta C_{\text{p},i}^{\text{ls}}\mathrm{d}T - \frac{1}{RT}\int_{T_i^{\text{f}}}^{T}\frac{\Delta C_{\text{p},i}^{\text{ls}}}{T}\mathrm{d}T \tag{4}$$

where T_i^{f} and T_i^{tr} are the solid−liquid (fusion) and solid−solid transition temperatures of the pure component "i", respec-

https://doi.org/10.1021/acsomega.1c07072
ACS Omega 2022, 7, 16928−16938

tively. ΔH_i^f and ΔH_i^{tr} are the enthalpies of fusion and solid−solid transition of the pure component "i", respectively. $\Delta C_{p,i}^{ls}$ represents the difference between the heat capacities of component "i" in the liquid and solid phases. Correlations used for calculating the fusion temperature and solid−solid transition temperature are varied considering even or odd carbon numbers of n-alkanes[6] and will be described using eqs 5−9.

- n-alkanes with an even carbon number.[6]
  For $C_{10} < C_n \leq C_{42}$

$$T^f(K) = 0.0031C_n^3 - 0.3458C_n^2 + 14.277C_n + 137.73 \quad (5)$$

  T^f indicates the fusion temperature.
  For $C_{22} \leq C_n \leq C_{42}$

$$T^{tr}(K) = 0.0032C_n^3 - 0.3249C_n^2 + 12.78C_n + 154.19 + \ln(C_n) \quad (6)$$

  T^{tr} denotes the transition temperature.
  Others

$$T^{tr}(K) = T^f(K) \quad (7)$$

- n-alkanes with an odd carbon number.[6]
  For $C_9 < C_n \leq C_{43}$

$$T^f(K) = 0.0122C_n^2 - 2.0861C_n - \frac{755.598}{C_n} + 76.2189\ln(C_n) + 156.9 \quad (8)$$

$$T^{tr}(K) = 0.0039C_n^3 - 0.4239C_n^2 + 17.28C_n - \ln(C_n) + 95.4 \quad (9)$$

  Correlations used for calculating the fusion heat and enthalpy of solid−solid transitions, which are a function of fusion temperature and molecular weight, are given by[6]
- n-alkanes with an even carbon number.[6]
  For $C_n \leq C_{20}$

$$\Delta H^f(\text{cal mol}^{-1}) = 0.180M_w \times T^f + 522.7 \quad (10)$$

  ΔH^f describes the fusion heat[6]

$$\Delta H^{tr}(\text{cal mol}^{-1}) = 0 \quad (11)$$

  ΔH^{tr} stands for the enthalpy of solid−solid transitions.
- n-alkanes with an odd carbon number.[6]
  For $C_9 < C_n \leq C_{43}$

$$\Delta H^f(\text{cal mol}^{-1}) = 0.74(0.167M_w \times T^f + 432.47) \quad (12)$$

$$\Delta H^{tr}(\text{cal mol}^{-1}) = 0.26(0.167M_w \times T^f + 432.47) \quad (13)$$

  ΔC_{p_i}, the specific heat capacity difference for component "i" is calculated using the following correlation[22]

$$\Delta C_{p_i}(\text{cal mol}^{-1}) = 0.3033M_{w_i} - 4.635 \times 10^{-4}M_{w_i} \times T \quad (14)$$

In eqs 5, 6, 8, and 9, C_n represents the carbon number of each component. Molecular weights, critical temperatures, and acentric factors of all components are reported in Table 4.

Table 4. Molecular Weights, Critical Temperatures, and Acentric Factors of the Components Used in This Study[34a,b,c]

	M_w (g mol^{-1})	T_c (K)	ω
n-C_{11}	156.308	639	0.5303
n-C_{14}	198.388	693	0.6430
n-C_{16}	226.441	723	0.7174
n-C_{18}	254.494	747	0.8114

[a] M_w: molecular weight. [b] T_c: critical temperature. [c] ω: acentric factor.

By incorporating eqs 1−4, the solid−liquid equilibrium ratio of component "i", K_i^{sl}, can be obtained[11,29]

$$K_i^{sl} = \frac{x_i^s}{x_i^l} = \frac{\gamma_i^l f_{pure,i}^l}{\gamma_i^s f_{pure,i}^s} \quad (15)$$

4.3.2. Thermodynamic Modeling: γ−φ Approach. In this approach, the nonidealities of the solid phase and the liquid phase are calculated using the activity coefficient models and PC-SAFT EoS,[28] respectively. The K_i^{sl} is computed as follows[11]

$$K_i^{sl} = \frac{x_i^s}{x_i^l} = \frac{\varphi_i^l P}{\gamma_i^s f_{pure,i}^s} \quad (16)$$

In eq 16, φ_i^l stands for the fugacity coefficient of component "i" in the liquid phase that can be calculated using PC-SAFT EoS[28]

$$\ln(\varphi_i^l) = \left[\frac{\partial(na^{res})}{\partial n_i}\right]_{T,\rho,n_j\neq i} + z - 1 - \ln(z) \quad (17)$$

In eq 17, a^{res} represents the reduced residual Helmholtz free energy, and z denotes the compressibility factor. Subscript n_j indicates that all mole numbers except n_i are held constant. In PC-SAFT EoS,[28] when no associating and polar forces exist, a^{res} and z can be written as follows[28]

$$a^{res} = a^{hc} + a^{disp} \quad (18)$$

$$z = z^{hc} + z^{disp} \quad (19)$$

In eqs 18 and 19, the superscript hc expresses the hard-chain molecules and superscript disp is the dispersive force contribution. The details of PC-SAFT EoS[28] are presented in previous studies.[28,30,31,35] The input parameters of the models are reported in Table 5. In this study, the binary interaction parameter, k_{ij}, is set to zero.[28,36]

5. ACTIVITY COEFFICIENT MODELS

5.1. Regular Solution Theory. Some researchers have applied the regular solution theory[19] to characterize the nonideality behaviors of paraffin wax mixtures.[19,23,29,37] In this approach, the activity coefficient is defined by the following correlation[19,25]

$$\ln\gamma_i = \frac{v_i(\bar{\delta} - \delta_i)^2}{RT} \quad (20)$$

https://doi.org/10.1021/acsomega.1c07072
ACS Omega 2022, 7, 16928−16938

Table 5. Input Parameters Used in This Work

		n-C_{11}	n-C_{14}	n-C_{16}	n-C_{18}
PC-SAFT EoS[28]	m	4.9082	5.9002	6.6485	7.3271
	σ (Å)	3.8893	3.9396	3.9552	3.9668
	ϵ/k (K)	248.82	254.21	254.70	256.20
regular solution theory[19]	δ^l (cal cm^{-3})$^{0.5}$	7.6773	7.8199	7.8989	7.9686
	δ^s (cal cm^{-3})$^{0.5}$	11.1048	12.4946	13.2641	13.9429
p.UNIQUAC[24]	r	1.1672	1.4672	1.6672	1.8672
	q	1.2141	1.5141	1.7141	1.9141
UNIFAC[25]	r	7.8718	9.8950	11.2438	12.5926
	q	6.5560	8.1760	9.2560	10.3360

where δ is the solubility parameter. Pedersen et al.[23] proposed two separate correlations to calculate the liquid and solid solubility parameters.

$$\delta_i^l = 7.41 + 0.5149\,(\ln C_{ni} - \ln 7) \tag{21}$$

$$\delta_i^s = 8.5 + 5.763\,(\ln C_{ni} - \ln 7) \tag{22}$$

δ_i^l and δ_i^s are input parameters for regular solution theory[19] that were calculated for all components (Table 5). v_i and $\bar{\delta}$ are the molar volume and average solubility parameters, respectively. In this work, the molar volumes of both phases are considered to be equal.[19,25]

$$\bar{\delta}_i = \sum \varphi_i \delta_i \tag{23}$$

$$v_i^l = v_i^s = \frac{M_{w_i}}{d_{i,25}^l} \tag{24}$$

$$\varphi_i^l = \frac{x_i^l v_i^l}{\sum x_i^l v_i^l} \tag{25}$$

$$\varphi_i^s = \frac{x_i^s v_i^s}{\sum x_i^s v_i^s} \tag{26}$$

where φ_i^l and φ_i^s are the liquid- and solid-phase volume fractions of component "i", respectively. The following correlation, which is molecular-weight (M_w)-dependent, is presented to compute the density of each component at 25 °C ($d_{i,25}^l$).[38]

$$d_{i,25}^l = 0.8155 + 0.6272 \times 10^{-4} M_{w_i} - \frac{13.06}{M_{w_i}} \tag{27}$$

5.2. Predictive Wilson Model. Another model applied to calculate the activity coefficients of n-alkane mixture components is predictive Wilson (p.Wilson).[20]

$$\ln \gamma_i = 1 - \ln\left(\sum_{j=1}^{n} x_j \Lambda_{ij}\right) - \sum_{k'=1}^{n} \frac{x_{k'} \Lambda_{k'i}}{\sum_{j=1}^{n} x_j \Lambda_{k'j}} \tag{28}$$

where n represents the number of components and Λ_{ij} is the interaction parameter between "i" and "j" molecules, which is calculated by the following relation[14]

$$\Lambda_{ij} = \exp\left(-\frac{\lambda_{ij} - \lambda_{ii}}{RT}\right) \tag{29}$$

The characteristic interaction energy that exists between two identical molecules, λ_{ii}, depends on the sublimation enthalpy ($\Delta H_{sub,i}$) and temperature.[20]

$$\lambda_{ii} = -\frac{2}{Z}(\Delta H_{sub,i} - RT) \tag{30}$$

The alkyl chains in the wax lead to an orthorhombic structure creation.[22,39,40] As a result, the coordination number, Z, is set to 6 for n-alkanes in the orthorhombic phase.[20] The sublimation enthalpy of pure n-alkanes is estimated by summing the component latent heats of the solid−solid transition (ΔH^{tr}), melting (ΔH^f), and vaporization (ΔH^{vap})[19]

$$\Delta H_{sub,i} = \Delta H_i^{vap} + \Delta H_i^f + \Delta H_i^{tr} \tag{31}$$

The correlation of Morgan and Kobayashi to calculate the enthalpy of vaporization is given as follows[41]

$$\frac{\Delta H_i^{vap}}{RT_c} = \Delta H_v^{(0)} + \omega \Delta H_v^{(1)} + \omega^2 \Delta H_v^{(2)} \tag{32}$$

$$\Delta H_v^{(0)} = 5.2804x'^{0.3333} + 12.865x'^{0.8333} + 1.171x'^{1.2083} - 13.116x' + 0.485x'^2 - 1.088x'^3 \tag{33}$$

$$\Delta H_v^{(1)} = 0.800x'^{0.3333} + 273.23x'^{0.8333} + 465.08x'^{1.2083} - 638.51x' - 145.12x'^2 + 74.049x'^3 \tag{34}$$

$$\Delta H_v^{(2)} = 7.2543x'^{0.3333} - 346.35x'^{0.8333} - 610.48x'^{1.2083} + 839.89x' + 160.05x'^2 - 50.71x'^3 \tag{35}$$

$$x' = \left(1 - \frac{T}{T_c}\right) \tag{36}$$

In eq 36, T_c represents the critical temperature. The pair interaction energies between nonidentical molecules ("i" and "j") are equal to those between two identical molecules with a shorter chain (j) of pair ij.[42]

$$\lambda_{ij} = \lambda_{ji} = \lambda_{jj} \tag{37}$$

5.3. Predictive UNIQUAC Model. The predictive UNIQUAC (p.UNIQUAC) model[24] comprises two terms: combinatorial and residual. The first term is an entropic term that computes the molecules' differences in shape, structure, and size. The second term is an enthalpic term that explains the energetic interaction between the various molecules.[24]

$$\ln \gamma_i = \ln \gamma_i^{comb} + \ln \gamma_i^{res} \tag{38}$$

$$\ln \gamma_i^{comb} = \ln\left(\frac{\Phi_i}{x_i}\right) + 1 - \left(\frac{\Phi_i}{x_i}\right) - \frac{Z}{2} q_i \left[\ln\left(\frac{\Phi_i}{\theta_i}\right) + 1 - \frac{\Phi_i}{\theta_i}\right] \tag{39}$$

https://doi.org/10.1021/acsomega.1c07072
ACS Omega 2022, 7, 16928−16938

$$\ln \gamma_i^{res} = q_i\left[1 - \ln\left(\sum_{j=1}^{n} \theta_j \tau_{ji}\right) - \sum_{j=1}^{n} \frac{\theta_j \tau_{ij}}{\sum_{k'=1}^{n} \theta_{k'} \tau_{k'j}}\right] \quad (40)$$

$$\tau_{ji} = \exp\left(-\frac{\lambda_{ji} - \lambda_{ii}}{q_i RT}\right) \quad (41)$$

The pair interaction energies are calculated in the same way as for the p.Wilson model.[24]

$$\Phi_i = \frac{x_i r_i}{\sum_{j=1}^{n} x_j r_j} \quad (42)$$

$$\theta_i = \frac{x_i q_i}{\sum_{j=1}^{n} x_j q_j} \quad (43)$$

In eqs 42 and 43, Φ_i and θ_i are segment and area fractions, respectively. The structural parameters of size, r_i, and external surface, q_i, can be obtained from the following relation[24]

$$r_i = 0.1C_{ni} + 0.0672 \quad (44)$$

$$q_i = 0.1C_{ni} + 0.1141 \quad (45)$$

r_i and q_i parameters are the calculated input data for the p.UNIQUAC model that are presented in Table 5.

5.4. UNIFAC Model. The UNIFAC model[25] is another model to demonstrate the nonideality of wax mixtures containing *n*-alkanes. This model also consists of two parts: combinatorial and residual. In this study, the combinatorial term is only used and the residual term is eliminated.[43−45]

$$\ln \gamma_i = \ln\left(\frac{\Phi_i}{x_i}\right) + 1 - \left(\frac{\Phi_i}{x_i}\right) - \frac{Z}{2} q_i\left(\ln\left(\frac{\Phi_i}{\theta_i}\right) + 1 - \frac{\Phi_i}{\theta_i}\right) \quad (46)$$

The segment fraction, Φ_i, and the area fraction, θ_i, are determined by eqs 42 and 43, respectively. The structural parameters, r_i and q_i, are calculated as follows[43]

$$r_i = 0.6744C_{ni} + 0.4534 \quad (47)$$

$$q_i = 0.54C_{ni} + 0.616 \quad (48)$$

The values of these parameters, which are the input data of the UNIFAC model,[25] are calculated for all components and are reported in Table 5.

AUTHOR INFORMATION

Corresponding Authors

Jafar Javanmardi − *Department of Chemical, Petroleum and Gas Engineering, Shiraz University of Technology, Shiraz 71557-13876, Iran*; Email: Javanmardi@sutech.ac.ir

Amir H. Mohammadi − *Discipline of Chemical Engineering, School of Engineering, University of KwaZulu-Natal, Durban 4041, South Africa*; orcid.org/0000-0002-2947-1135; Email: amir_h_mohammadi@yahoo.com

Authors

Fatemeh Shariatrad − *Department of Chemical, Petroleum and Gas Engineering, Shiraz University of Technology, Shiraz 71557-13876, Iran*

Ali Rasoolzadeh − *Department of Chemical, Petroleum and Gas Engineering, Shiraz University of Technology, Shiraz 71557-13876, Iran; Chemical Engineering Department, Lamerd Higher Education Center, Lamerd 74341-67441, Iran*

Complete contact information is available at: https://pubs.acs.org/10.1021/acsomega.1c07072

Funding

This research received no specific grant from any funding agency in the public, commercial, or not-for-profit sectors.

Notes

The authors declare no competing financial interest.

ACKNOWLEDGMENTS

Support of this work by the Shiraz University of Technology is highly acknowledged.

NOMENCLATURE

AAD	average absolute deviation
C_n	carbon number
C_p	specific heat capacity
d	density
f	fugacity
a^{res}	reduced residual Helmholtz free energy
H	enthalpy
i	component counter
j	component counter
k	Boltzmann constant
k'	component counter
k_{ij}	binary interaction parameter
K	equilibrium constant
m	number of segments per chain
M_w	molecular weight
n	number of components
P	pressure
q	molecular external surface parameter
r	molecular size parameter
R	Universal gas constant
T	temperature
T_c	critical temperature
v	molar volume
x	mole fraction
Z	coordination number
z	compressibility factor

GREEK CHARACTERS

ϵ	depth of pair potential
γ	activity coefficient
δ	solubility parameter
$\bar{\delta}$	average solubility parameter
Δ	variation
θ	area fraction
λ	interaction energy
σ	segment diameter
Λ	interaction parameter
τ	characteristic energy parameter
φ	volume fraction
Φ	segment fraction
ω	acentric factor
φ_i^l	fugacity coefficient of component "i" in the liquid

SUPERSCRIPTS

Cal	calculated
comb	combinatorial

https://doi.org/10.1021/acsomega.1c07072
ACS Omega 2022, 7, 16928−16938

Exp	experimental
f	fusion
l	liquid
res	residual
s	solid
tot	total
tr	transition
vap	vaporization

SUBSCRIPTS

i	component number
j	component number
k′	component number
n	component number
sub	sublimation

REFERENCES

(1) Zou, C.; Zhao, Q.; Zhang, G.; Xiong, B. Energy Revolution: From a Fossil Energy Era to a New Energy Era. *Nat. Gas Ind. B* **2016**, *3*, 1−11.

(2) Hammami, A.; Mehrotra, A. K. Non-Isothermal Crystallization Kinetics of N-Paraffins: Comparison of Even-Numbered and Odd-Numbered Normal Alkanes. *Thermochim. Acta* **1993**, *215*, 197−209.

(3) Vieira, L. C.; Buchuid, M. B.; Lucas, E. F. Evaluation of Pressure on the Crystallization of Waxes Using Microcalorimetry. *J. Therm. Anal. Calorim.* **2013**, *111*, 583−588.

(4) Hammami, A.; Raines, M. A. Paraffin Deposition from Crude Oils: Comparison of Laboratory Results with Field Data. *SPE J.* **1999**, *4*, 9−18.

(5) Kasumu, A. S.; Arumugam, S.; Mehrotra, A. K. Effect of Cooling Rate on the Wax Precipitation Temperature of "Waxy" Mixtures. *Fuel* **2013**, *103*, 1144−1147.

(6) Ji, H.-Y.; Tohidi, B.; Danesh, A.; Todd, A. C. Wax Phase Equilibria: Developing a Thermodynamic Model Using a Systematic Approach. *Fluid Phase Equilib.* **2004**, *216*, 201−217.

(7) Hammami, A.; Mehrotra, A. K. Liquid-Solid-Solid Thermal Behaviour of N-$C_{44}H_{90}$ + N-$C_{50}H_{102}$ and N-$C_{25}H_{52}$ + N-$C_{28}H_{58}$ Paraffinic Binary Mixtures. *Fluid Phase Equilib.* **1995**, *111*, 253−272.

(8) Tiwary, D.; Mehrotra, A. K. Phase Transformation and Rheological Behaviour of Highly Paraffinic "Waxy" Mixtures. *Can. J. Chem. Eng.* **2004**, *82*, 162−174.

(9) Bhat, N. V.; Mehrotra, A. K. Measurement and Prediction of the Phase Behavior of Wax− Solvent Mixtures: Significance of the Wax Disappearance Temperature. *Ind. Eng. Chem. Res.* **2004**, *43*, 3451−3461.

(10) Nasrifar, K.; Kheshty, M. F. Effect of Pressure on the Solid−Liquid Equilibria of Synthetic Paraffin Mixtures Using Predictive Methods. *Fluid Phase Equilib.* **2011**, *310*, 111−119.

(11) Aftab, S.; Javanmardi, J.; Nasrifar, K. Experimental Investigation and Thermodynamic Modeling of Wax Disappearance Temperature for N-Undecane + N-Hexadecane + N-Octadecane and N-Tetradecane + N-Hexadecane + N-Octadecane Ternary Systems. *Fluid Phase Equilib.* **2015**, *403*, 70−77.

(12) Wang, K.-S.; Wu, C.-H.; Creek, J. L.; Shuler, P. J.; Tang, Y. Evaluation of Effects of Selected Wax Inhibitors on Wax Appearance and Disappearance Temperatures. *Pet. Sci. Technol.* **2003**, *21*, 359−368.

(13) Roenningsen, H. P.; Bjoerndal, B.; Baltzer Hansen, A.; Batsberg Pedersen, W. Wax Precipitation from North Sea Crude Oils: 1. Crystallization and Dissolution Temperatures, and Newtonian and Non-Newtonian Flow Properties. *Energy Fuels* **1991**, *5*, 895−908.

(14) Lira-Galeana, C.; Hammami, A. Wax Precipitation from Petroleum Fluids: A Review. *Dev. Pet. Sci.* **2000**, *40*, 557−608.

(15) Hammami, A.; Raines, M. A. Paraffin Deposition From Crude Oils: Comparison of Laboratory Results to Field Data. *SPE Annu. Tech. Conf. Exhib.* **1997**, No. 38776.

(16) Daridon, J.-L.; Pauly, J.; Milhet, M. High Pressure Solid−Liquid Phase Equilibria in Synthetic Waxes. *Phys. Chem. Chem. Phys.* **2002**, *4*, 4458−4461.

(17) Pauly, J.; Daridon, J.-L.; Coutinho, J. A. P. Solid Deposition as a Function of Temperature in the nC_{10} + (nC_{24}−nC_{25}−nC_{26}) System. *Fluid Phase Equilib.* **2004**, *224*, 237−244.

(18) Mansourpoor, M.; Azin, R.; Osfouri, S.; Izadpanah, A. A. Experimental Measurement and Modeling Study for Estimation of Wax Disappearance Temperature. *J. Dispersion Sci. Technol.* **2019**, *40*, 161−170.

(19) Won, K. W. Thermodynamics for Solid Solution-Liquid-Vapor Equilibria: Wax Phase Formation from Heavy Hydrocarbon Mixtures. *Fluid Phase Equilib.* **1986**, *30*, 265−279.

(20) Coutinho, J. A. P.; Stenby, E. H. Predictive Local Composition Models for Solid/Liquid Equilibrium in N-Alkane Systems: Wilson Equation for Multicomponent Systems. *Ind. Eng. Chem. Res.* **1996**, *35*, 918−925.

(21) Lira-Galeana, C.; Firoozabadi, A.; Prausnitz, J. M. Thermodynamics of Wax Precipitation in Petroleum Mixtures. *AIChE J.* **1996**, *42*, 239−248.

(22) Soave, G. Equilibrium constants from a modified Redlich-Kwong equation of state. *Chem. Eng.-Sci.* **1972**, *27*, 1197−1203.

(23) Pedersen, K. S.; Skovborg, P.; Roenningsen, H. P. Wax Precipitation from North Sea Crude Oils. 4. Thermodynamic Modeling. *Energy Fuels* **1991**, *5*, 924−932.

(24) Coutinho, J. A. P. Predictive UNIQUAC: A New Model for the Description of Multiphase Solid−Liquid Equilibria in Complex Hydrocarbon Mixtures. *Ind. Eng. Chem. Res.* **1998**, *37*, 4870−4875.

(25) Prausnitz, J. M.; Lichtenthaler, R. N.; de Azevedo, E. G. *Molecular Thermodynamics of Fluid-Phase Equilibria*, 3rd ed.; Pretince-Hall: New Jersey, 1999.

(26) Peng, D.-Y.; Robinson, D. B. A new two-constant equation of state. *Ind. Eng. Chem. Fundam.* **1976**, *15*, 59−64.

(27) Esmaeilzadeh, F.; Kaljahi, J. F.; Ghanaei, E. Investigation of Different Activity Coefficient Models in Thermodynamic Modeling of Wax Precipitation. *Fluid Phase Equilib.* **2006**, *248*, 7−18.

(28) Gross, J.; Sadowski, G. Perturbed-Chain SAFT: An Equation of State Based on a Perturbation Theory for Chain Molecules. *Ind. Eng. Chem. Res.* **2001**, *40*, 1244−1260.

(29) Parsa, S.; Javanmardi, J.; Aftab, S.; Nasrifar, K. Experimental Measurements and Thermodynamic Modeling of Wax Disappearance Temperature for the Binary Systems n-$C_{14}H_{30}$ + n-$C_{16}H_{34}$, n-$C_{16}H_{34}$ + n-$C_{18}H_{38}$ and n-$C_{11}H_{24}$ + n-$C_{18}H_{38}$. *Fluid Phase Equilib.* **2015**, *388*, 93−99.

(30) Nasrifar, K.; Tafazzol, A. H. Vapor-Liquid Equilibria of Acid Gas-Aqueous Ethanolamine Solutions Using the PC-SAFT Equation of State. *Ind. Eng. Chem. Res.* **2010**, *49*, 7620−7630.

(31) Nasrifar, K. A Perturbed-Chain SAFT Equation of State Applied to the Mixtures of Short and Long Chain N-Alkanes. *Ind. Eng. Chem. Res.* **2013**, *52*, 6582−6591.

(32) Shimura, T.; Kemp, A. I. S. Tetrahedral plot diagram: A Geometrical Solution for Quaternary Systems. American Mineralogist: Earth Planet. *Am. Mineral.* **2015**, *100*, 2545−2547.

(33) Coutinho, J. A. P.; Mirante, F.; Pauly, J. A New Predictive UNIQUAC for Modeling of Wax Formation in Hydrocarbon Fluids. *Fluid Phase Equilib.* **2006**, *247*, 8−17.

(34) Green, D. W.; Perry, R. H. *Perry's Chemical Engineer's Handbook*, 8th ed.; McGraw-Hill: USA, 2008.

(35) Parvaneh, K.; Rasoolzadeh, A.; Shariati, A. Modeling the Phase Behavior of Refrigerants with Ionic Liquids Using the QC-PC-SAFT Equation of State. *J. Mol. Liq.* **2019**, *274*, 497−504.

(36) Sa-ngawong, N.; Kangsadan, T.; Cheenkachorn, K.; Inwong, N.; Mahittikul, A. Study on Local Composition of Binary n-Alkane for Precise Estimation of Wax Disappearance Temperature. *Appl. Sci. Eng. Prog.* **2021**, *14*, 271−283.

(37) Yang, J.; Wang, W.; Shi, B.; Ma, Q.; Song, P.; Gong, J. Prediction of Wax Precipitation with New Modified Regular Solution Model. *Fluid Phase Equilib.* **2016**, *423*, 128−137.

https://doi.org/10.1021/acsomega.1c07072
ACS Omega 2022, 7, 16928−16938

(38) Won, K. W. In *Continuous Thermodynamics for Solid-Liquid Equilibria: Wax Formation from Heavy Hydrocarbon Mixtures*, AIChE Spring National Meeting, 1986.
(39) Chevallier, V.; Briard, A. J.; Petitjean, D.; Hubert, N.; Bouroukba, M.; Dirand, M. Influence of the Distribution General Shape of N-Alkane Molar Concentrations on the Structural State of Multi-Alkane Mixtures. *Mol. Cryst. Liq. Cryst. Sci. Technol., Sect. A* **2000**, *350*, 273−291.
(40) Dirand, M.; Chevallier, V.; Provost, E.; Bouroukba, M.; Petitjean, D. Multicomponent Paraffin Waxes and Petroleum Solid Deposits: Structural and Thermodynamic State. *Fuel* **1998**, *77*, 1253−1260.
(41) Morgan, D. L.; Kobayashi, R. Extension of Pitzer CSP Models for Vapor Pressures and Heats of Vaporization to Long-Chain Hydrocarbons. *Fluid Phase Equilib.* **1994**, *94*, 51−87.
(42) Coutinho, J. A. P.; Knudsen, K.; Andersen, S. I.; Stenby, E. H. A Local Composition Model for Paraffinic Solid Solutions. *Chem. Eng. Sci.* **1996**, *51*, 3273−3282.
(43) Fredenslund, A.; Jones, R. L.; Prausnitz, J. M. Group-Contribution Estimation of Activity Coefficients in Nonideal Liquid Mixtures. *AIChE J.* **1975**, *21*, 1086−1099.
(44) Larsen, B. L.; Rasmussen, P.; Fredenslund, A. A Modified UNIFAC Group-Contribution Model for Prediction of Phase Equilibria and Heats of Mixing. *Ind. Eng. Chem. Res.* **1987**, *26*, 2274−2286.
(45) Gao, W.; Robinson, R. L., Jr.; Gasem, K. A. M. Improved Correlations for Heavy N-paraffin Physical Properties. *Fluid Phase Equilib.* **2001**, *179*, 207−216.

https://doi.org/10.1021/acsomega.1c07072
ACS Omega 2022, 7, 16928−16938